Radio Science, Volume 25, Number 1, Pages 37–48, January–February 1990

Mean square slopes of the wind-disturbed water surface, their magnitude, directionality, and composition

Jin Wu

Air-Sea Interaction Laboratory, College of Marine Studies, University of Delaware, Lewes

(Received January 30, 1989; revised November 20, 1989; accepted November 22, 1989.)

Available laboratory and field data on fine structures of the wind-disturbed water surface are reviewed and analyzed to deduce the quantitative variation of directional mean square slopes with the wind condition. The mean square slope is associated with the wind-friction velocity, with its maximum component in the upwind-downwind direction and minimum component in the crosswind direction. Its angular distribution is suggested to follow an elliptical function. Spectral compositions of fine surface structures are estimated; in the field, gravity wave components contribute the most at low winds ($U_{10} < 7$ m s^{-1} or $u_* < 20$ cm s^{-1}) and capillary components at high winds; in laboratory tanks, gravity components are relatively much more important. These along with the other features are used to explain discrepancies between laboratory and field results as well as those within each group.

1. INTRODUCTION

Fine structures of ocean waves, a central subject in studies of the air-sea interaction, have attracted an ever-increasing attention lately, as they govern radar backscattering and radiometric emission of microwaves from the sea surface [*Moore*, 1985]. Many investigations have been performed in laboratory wind-wave tanks [*Cox*, 1958; *Wu*, 1971, 1977; *Long and Huang*, 1976; *Haimbach*, 1985; *Haimbach and Wu*, 1986] and in the field [*Cox and Munk*, 1956; *Hughes et al.*, 1977; *Tang and Shemdin*, 1983; *Haimbach and Wu*, 1985], seeking to quantify these structures best described by the slope statistics. It is generally considered that ocean ripples reaching quite readily an equilibrium state with the wind can be modeled in laboratory tanks and that the mean square water-surface slopes obtained at drastically different fetches in laboratory tanks and the field can be scaled on the basis of wind-friction velocity. There are, however, large discrepancies between laboratory and field results as well as among measurements within each group. In the present article, laboratory and field results were reviewed first separately to deal with those discrepancies, and then combined to deal with their quantification. Finally, formulae were proposed for both laboratory and field conditions to express the mean square slope and directional spreading of fine surface structures in terms of the wind-friction velocity.

Paper number 89RS03580.
0048-6604/90/89RS-03580$08.00

2. REPORTED RESULTS

Field investigations

Sun-glitter reflection results. *Cox and Munk* [1956] deduced slopes of the sea surface from the brightness distribution in photographs of Sun glitters on the sea surface in the Hawaiian area. Mean square slopes $\overline{s^2}$ were obtained from these distributions along with the ratio between the crosswind and upwind-downwind components $\overline{s_c^2}/\overline{s_l^2}$; these results are reproduced in Figures 1*a* and 1*d*, in which $U_{12.5}$ is the wind velocity measured at 12.5 m above the mean sea surface. Cox and Munk suggested a linear variation of the mean square slope with wind velocity,

$$\overline{s^2} = 0.003 + 5.12 \times 10^{-3} U_{12.5} \pm 0.04 \qquad (1)$$

where $U_{12.5}$ is expressed in meters per second.

Laser-optic refraction results. An optical technique sensing from above the water-surface slope through its defraction of a submerged, vertically upward laser beam was developed by *Hughes et al.* [1977]. The instrument was suspended on a crane ahead the bow of a vessel; a large lens above the water surface was used to collect the refracted beam and focus it onto a sensor. The vessel thus served essentially as a follower of large ocean

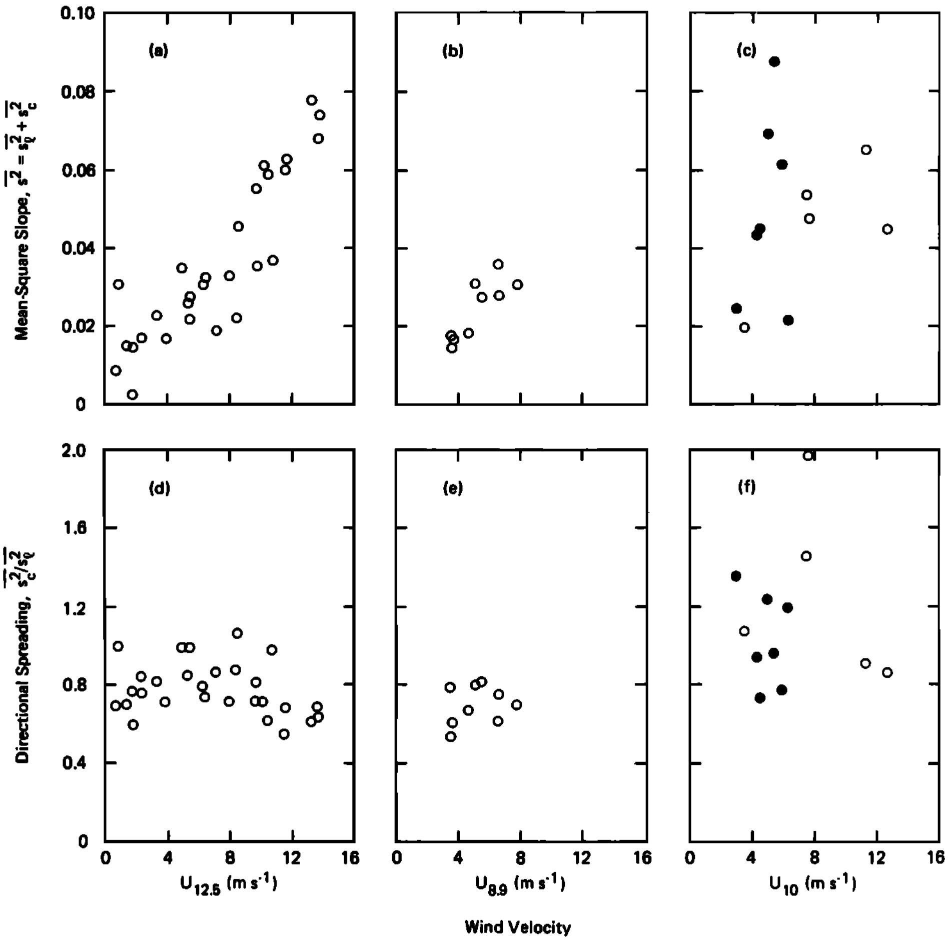

Fig. 1. Sea-surface slope statistics measured by *Cox and Munk* [1956] in (*a*) and (*d*), by *Hughes et al.* [1977] in (*b*) and (*e*), and by *Tang and Shemdin* [1983] in (*c*) and (*f*). The open circles in (*c*) and (*f*) are for cases with a well-defined wave spectrum as in other cases, and the solid circles are for cases with the mixed sea.

waves. Their system experienced, however, large signal losses up to about 24% of the sampling in some cases, with an average loss at about 10%. The experiments were conducted in the Bute inlet and Strait of Georgia on the west coast of Canada, at relatively low winds of 3.5–7.8 m s^{-1} and under mostly stable atmospheric conditions with the air-sea temperature difference varying between 1° and 10°C. Wind velocities were measured at two elevations of 8.9 and 21.7 m above the mean sea surface; their results on the mean square slope are plotted versus $U_{8.9}$ in Figures 1*b* and 1*e*.

A similar device was used more recently by *Tang and Shemdin* [1983] on the Noordwijk Research Tower, located 10 km offshore from the coast of Holland in a water depth of about 18 m. The sensor in this case, however, was mounted on a mechanical wave follower. Their results were rather scattered; this was considered to be caused mainly by differences in long-wave structures. They went on to classify the sea surface into two categories: "well-defined peak" and "mixed sea", corresponding respectively to cases with and without a well-defined peak in the elevation spectrum of surface waves. However, there was only one case which actually belonged to the so-called mixed sea (Tang, personal communication, 1989); more will be discussed in a later section. Variations of the mean square slope with wind velocity were found to be rather different for these two cases; see the results reproduced in Figures 1*c* and 1*f*. The elevation of wind-velocity measurements in Tang and Shemdin's investigation was not available and was considered here as 10 m.

Laser-optic reflection results. Probability density functions of directional sea-surface slopes were measured by *Haimbach and Wu* [1985] with an optical scanner. Rotating at 2000 rpm, the sensor directed a laser beam to scan from above the sea surface; successive series of scans were taken, with the laser beam in each series being set at a given angle from the vertical. The light was reflected back to the scanner when the illuminated spot on the sea surface, 1.2 mm in diameter, was normal to the beam. Directional distributions of sea-surface slopes could therefore be compiled from frequencies of their occurrences to determine the mean square slope and its directional spreading. Results of a preliminary nature were obtained and found to compare reasonably well with those of *Cox and Munk* [1956].

Laboratory investigations

Light-refraction results. *Cox* [1958] reported the first set of experiments with the light-refraction technique in a small wind-wave tank. Frequency spectra of surface slopes were reported. In his arrangement the light source was above and the receiver below the water surface. Cox's measurements, however, were influenced by undulations of the water surface and were also performed at rather short fetches, 1.5, 2.1, and 3.2 m. In addition, the wind-friction velocity was not measured; it is therefore difficult to compare his results with those of other laboratory studies discussed hereafter.

Long and Huang [1976] adopted the same technique but with different kinds of light source and receiver, so arranged to avoid the influence of water-surface undulations. The slope resolution of their unit was, however, at increments of as large as 4°. Measurements were performed at three fetches, 2.6, 4.7, and 6.7 m; the results of mean square slopes showed a general increase with fetch. Those collected at the longest fetch are reproduced in Figure 2*a*, where u_* is the wind-friction velocity. The water depth in their experiment was unspecified.

Two-dimensional slope spectra of the wind-disturbed water surface were measured by *Haimbach* [1985] with a laser and computer-interfaced photodiode-matrix camera system in a large wind-wave tank operated at a water depth of 75 cm. The laser

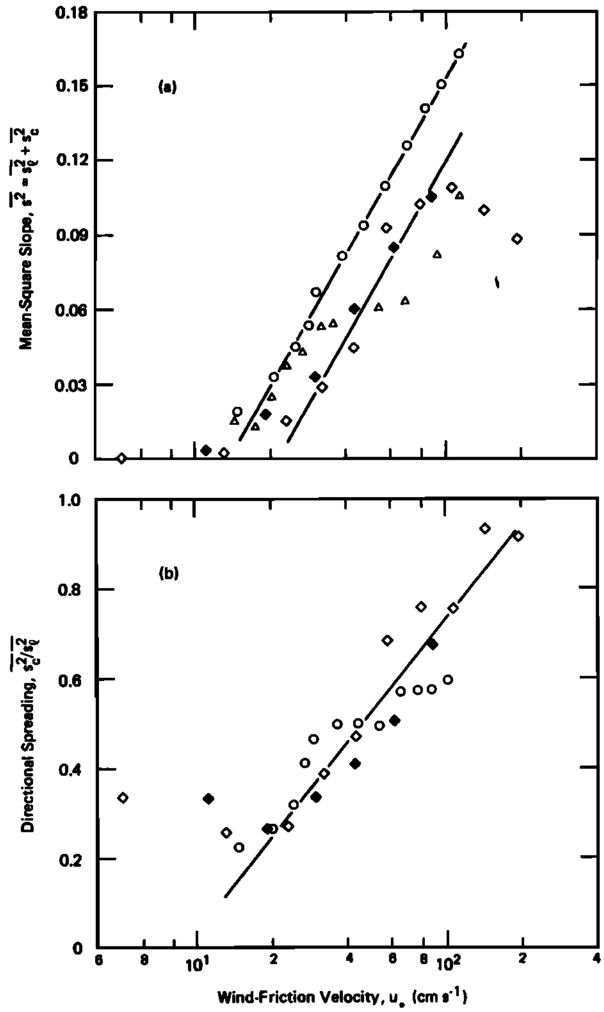

Fig. 2. Laboratory measurements of wind-wave slope statistics. The results are from *Long and Huang* [1976] (open triangles); *Wu* [1977] (open circles); *Haimbach and Wu* [1986] (closed diamonds); and *Haimbach* [1985] (open diamonds).

beam directed vertically upward was refracted by the water surface to project an image onto a horizontal screen, which was installed as a part of the tank cover at a fetch of 22 m. The image of projected beam on the screen was recorded by the matrix camera operated at a rate of 400 frames s^{-1} and was processed to obtain the surface slope. A time series of essentially continuous slope signals was then compiled to determine the slope spectrum, from which the mean square slope was calculated. His experiments were also conducted over a much wider range of wind velocities in comparison with other laboratory studies. The mean square slopes and ratios between their crosswind and upwind-downwind components are presented in Figures 2*a* and 2*b*, respectively.

Light-reflection results. An optical instrument utilizing the light reflection principle was used by *Wu* [1971] to measure the slope and curvature distributions in the upwind-downwind direction. This instrument having a resolution of 1° was subsequently modified [*Wu*, 1977] to measure these distributions along two principal axes (upwind-downwind and crosswind). Results obtained at a fetch of 11 m under various wind velocities were reported; the operating water depth was 1.24 m. Along both axes the slope distributions were found to be nearly Gaussian, and the components of mean square slope varied with the logarithm of wind-friction velocity. As the wind velocity increased, the ratio between crosswind and upwind-downwind components increased from a value of 1/5 to 4/5. The average radius of curvature was found to vary inversely with the wind-friction velocity; the ratio between two curvature components had a value of unity at all wind velocities, indicating that the wind-disturbed water surface is isotropic on the smallest scale. The mean square slopes and the ratios between crosswind and upwind-downwind components are presented in Figures 2*a* and 2*b*, respectively.

The scanner described earlier [*Haimbach and Wu*, 1985] was also used to measure fine structures in the same tank used by *Haimbach* [1985]. The total mean square slope and the ratio between two principal components reported by *Haimbach and Wu* [1986] are plotted versus the wind-friction velocity in Figures 2*a* and 2*b*.

Lines fitted to the data presented in Figures 2*a* and 2*b* will be discussed later.

3. COMPOSITIONS OF MEAN SQUARE SLOPES

Slope compositions in the field

Further interpretation of experimental results. The mean square slope of the sea surface can be related to the directional wave number spectrum $\psi(\mathbf{k})$ as [*Phillips*, 1977]

$$\overline{s^2} = \int_0^\infty k^2 \psi(\mathbf{k})\, d\mathbf{k} \qquad (2)$$

$$\psi(\mathbf{k}) = (B/\pi)k^{-4} \qquad k_\gamma > k > k_0$$
$$\psi(\mathbf{k}) = (B'/\pi)k^{-4} \qquad k_\nu > k > k_\gamma$$

where $\mathbf{k}$ and k, respectively, are the wave number vector and scalar, k_0 is at the spectral maximum, k_γ is where the effects of gravity and surface tension on the wave propagation are balanced, and k_ν is the neutrally stable wave number; B and B' are spectral coefficients for the gravity and capillary ranges, respectively.

Longuet-Higgins [1969] showed that the spectrum was not universal and associated its coefficient with the wave age. Subsequently, *Hasselmann et al.* [1973] related the spectral coefficient obtained during the Joint North Sea Wave Project to the nondimensional fetch. These are consistent results, as there is a unique relationship between the wave age and nondimensional fetch [*Wu*, 1985]. In the meantime, studies by *Toba* [1973], *Kitaigorodskii* [1983], and *Phillips* [1985] have demonstrated that the shape of spectrum following k^{-4}, as shown in (2), may no longer be attainable. Nonetheless, the k^{-4} spectrum may still serve as the asymptote of gravity-wave spectra being applicable at high-frequency waves [*Phillips*, 1985]. Moreover, much of the contribution to the mean square slope came from the capillary range, for which no revision of the k^{-4} spectrum has been proposed.

Mean square slopes measured by *Cox and Munk* [1956] are replotted in Figure 3*a* in the form suggested by (3) below. A portion of their measurements was conducted in the interior of a dense slick, where waves shorter than roughly a foot were observed visually to be absent. Consequently, for this portion of the data on fine sea-surface structures provided solely by gravity waves, we can rewrite (2) as

$$\overline{s^2} = B \ln\,[(U_{10}^2/g)k_s] \qquad (3)$$

in which the approximation $k_0 = g/U_{10}^2$ was substituted, with g being the gravitational acceleration and k_s the wave number of shortest waves over the slick surface. Fitting the above expression to the data, *Wu* [1972] obtained

$$B = 4.6 \times 10^{-3} \qquad \lambda_s = 2\pi/k_s = 38 \text{ cm} \qquad (4)$$

where λ_s is then the length of shortest waves over the slick surface, and its value is in a rather close agreement with the observation.

Relative to those obtained inside the slick, the

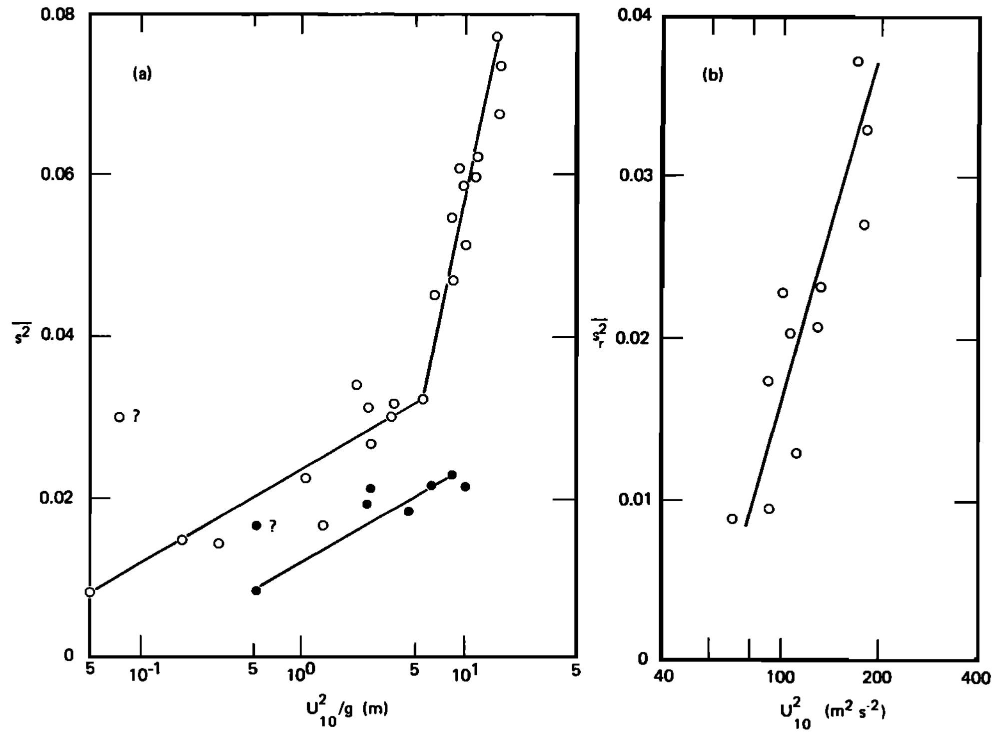

Fig. 3. Contributions of mean square sea-surface slopes by waves. The data obtained from the clean surface are shown in open circles, and from the slick surfaces data are shown in closed circles; only data at high wind velocities are shown in (*b*). The two data points clearly deviating from the main group and indicated by question marks were ignored in the curve fitting. All the data were obtained by *Cox and Munk* [1956].

data from the clean sea surface at low winds are seen in Figure 3*a* to have an almost upward parallel shift. The mean square slope corresponding to this shift, about 0.0115, must be associated with wave components having their wave number greater than k_s. Consequently, the cutoff wave number k_c at low winds was obtained by *Wu* [1972] from (3) and (4), provided, of course, that k_c is smaller than k_γ,

$$0.0046 \ln (k_c/k_s) = 0.0115 \qquad k_c = 2.5 \text{ cm}^{-1} \qquad (5)$$

The value of k_c is seen indeed smaller than k_γ, which is about 3.6 cm^{-1}. (The wave component dividing the gravity and capillary ranges has the wavelength of 1.73 cm, or the frequency of 13.4 Hz.) The closeness of these two values was interpreted to indicate that the portion of mean square slopes at high winds above the extension of the line fitted to the clean-surface data at low winds, $\overline{s_r^2}$, came from wave components in the capillary range [*Wu*, 1972].

Accepting the above argument we can write for high winds

$$\overline{s^2} - B \ln (k_c U_{10}^2/g) = \overline{s_r^2} = B' \ln (k_f/k_\gamma) \qquad (6)$$

in which k_f is used to replace k_ν, with k_f approaching k_ν as a limit. The spectral coefficient B' can now be determined independently from the slope of line fitted to the data replotted in Figure 3*b*, $B' = 3.15 \times 10^{-2}$. The latter is much greater than the coefficient B for the gravity range; consequently, when the capillary range started to make a contribution at wind velocities greater than 7 m s^{-1}, the mean square slope increased rapidly as illustrated in Figure 3*a*.

Spectral composition of mean square slopes. The spectral composition of mean square slope shown in (2) along with spectral coefficients determined in the previous section are illustrated graphically in Figures 4*a* and 4*b*. The transition

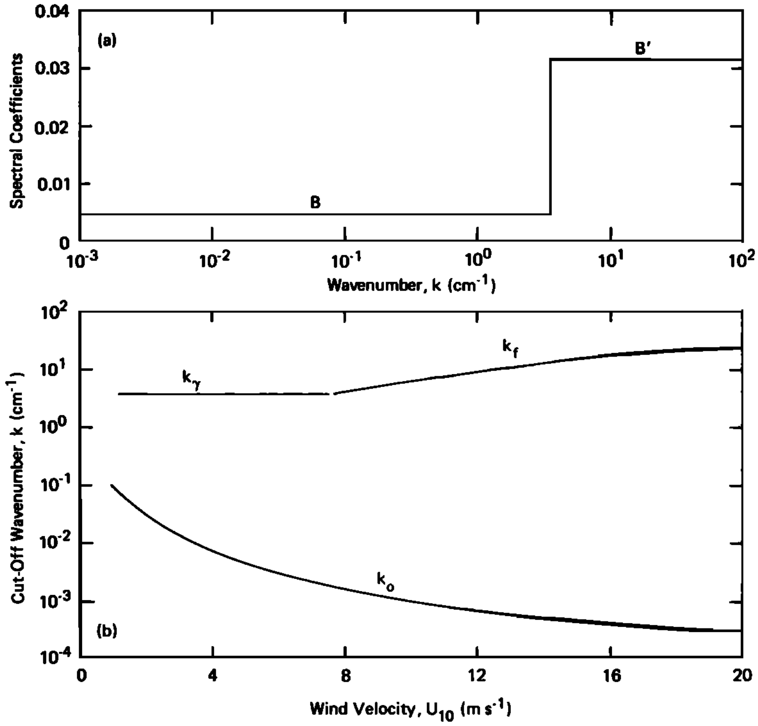

Fig. 4. Coefficients and cutoff wave numbers of directional wave number spectra at various wind velocities.

between B and B' regions, of course, should not be as sharp as that drawn in Figure 4a; this will be left to be resolved by future studies. The lower limit of the contribution to the mean square slope for all wind velocities comes from the spectral peak approximated by $k_0 = g/U_{10}^2$. The upper limit at low winds ($U_{10} < 7$ m s^{-1}) is at the wave number dividing gravity and surface tension influences on the wave propagation. At high winds the cutoff wave number can be obtained from (6)

$$k_f/k_\gamma = U_{10}^2 \exp(A/B') = 1.67 \times 10^{-2} U_{10}^2 \quad (7)$$

where A is the intercept of the line shown in Figure 3b, and U_{10} is expressed in m s^{-1}.

Considering that the line fitted to the data at low winds shown in Figure 3a represents the upper bound of contributions from the gravity ranges to the mean square slope, the relative contribution from capillary and gravity ranges $\overline{s_{cp}^2}/\overline{s_{gr}^2}$ was then obtained at various wind velocities. The latter were transferred to the wind-friction velocities by applying the formulae proposed by *Wu* [1986] to wind-velocity and temperature data of *Cox and Munk* [1956],

Unstable cases

$$C_s/C_{10} = \exp[0.614(-\Delta T/U_{10})^{5/3}] \quad (8a)$$

Stable cases

$$C_s/C_{10} = \exp[0.424(-\Delta T/U_{10})^{5/3}] \quad (8b)$$

where C_{10} and C_s, respectively, are the wind-stress coefficients under neutral and stable (or unstable) conditions, ΔT is the air-sea temperature difference in celsius, and U_{10} is expressed in meters per second. The wind-stress coefficient under neutral conditions suggested by *Wu* [1980] was also used,

$$C_{10} = (0.8 + 0.065 U_{10}) \times 10^{-3} \quad (9)$$

where U_{10} is again in meters per second. The results are shown in Figure 5 and illustrate quantitatively relative contributions of capillary and gravity ranges to fine sea-surface structures. The mean square slope is seen to be contributed mainly by the gravity range at low winds, and the capillary range starts to contribute at the wind velocity of about 7 m s^{-1}, corresponding to the wind-friction velocity of

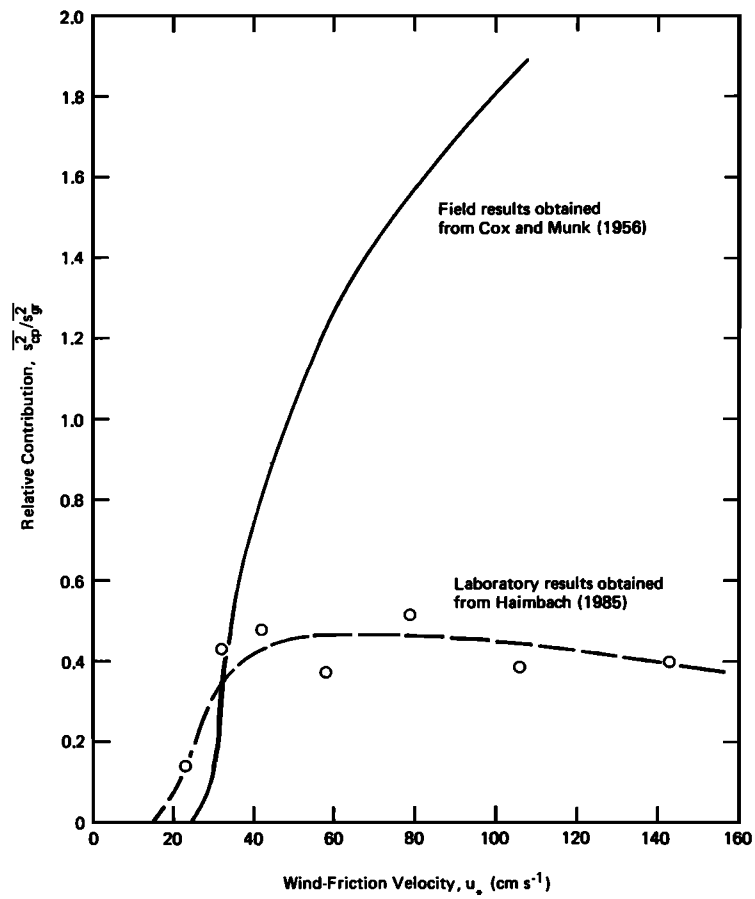

Fig. 5. Relative contributions of capillary and gravity ranges to fine structures of the wind-disturbed water surface.

about 25 cm s^{-1}. The latter contribution then rises sharply with the wind velocity. Both ranges make equal contributions at the wind velocity of 11.5 m s^{-1}, or the wind-friction velocity of 45 cm s^{-1}. At higher wind velocities the capillary range provides the major contribution. It is interesting to note that light winds generally prevail over the world's oceans [*Scully-Power*, 1986]; consequently, under most oceanic conditions, ripples are generally outside the capillary range [*Wu*, 1989].

Slope compositions in laboratory tanks

Frequency spectra of surface slopes. As discussed earlier, slope spectra of the wind-disturbed water surface were obtained by *Haimbach* [1985]. His results presented in the area preserving form are reproduced in Figure 6, where f and $S(f)$, respectively, are the apparent frequency of waves and the spectral density of slope spectrum. The term of apparent frequency is used to differentiate it from the true frequency, as the former measured with a stationary sensor was Doppler shifted by wind- and wave-induced drift currents. The frequency-weighted slope spectrum was suggested by Haimbach to consist of five regions. It suffices for the present purpose to identify only the following: (1) there is a spectral peak associated with that of the elevation spectrum, and this peak moves toward a lower frequency as the wind velocity increases; (2) there also exists a second but much broader peak at high frequencies; and (3) the upper frequency end of measurements is limited by the Nyquist frequency at about 200 Hz. Note that it is rather difficult to evaluate the shape of slope spectrum, as again the frequency was Doppler shifted.

Spectral composition of mean square

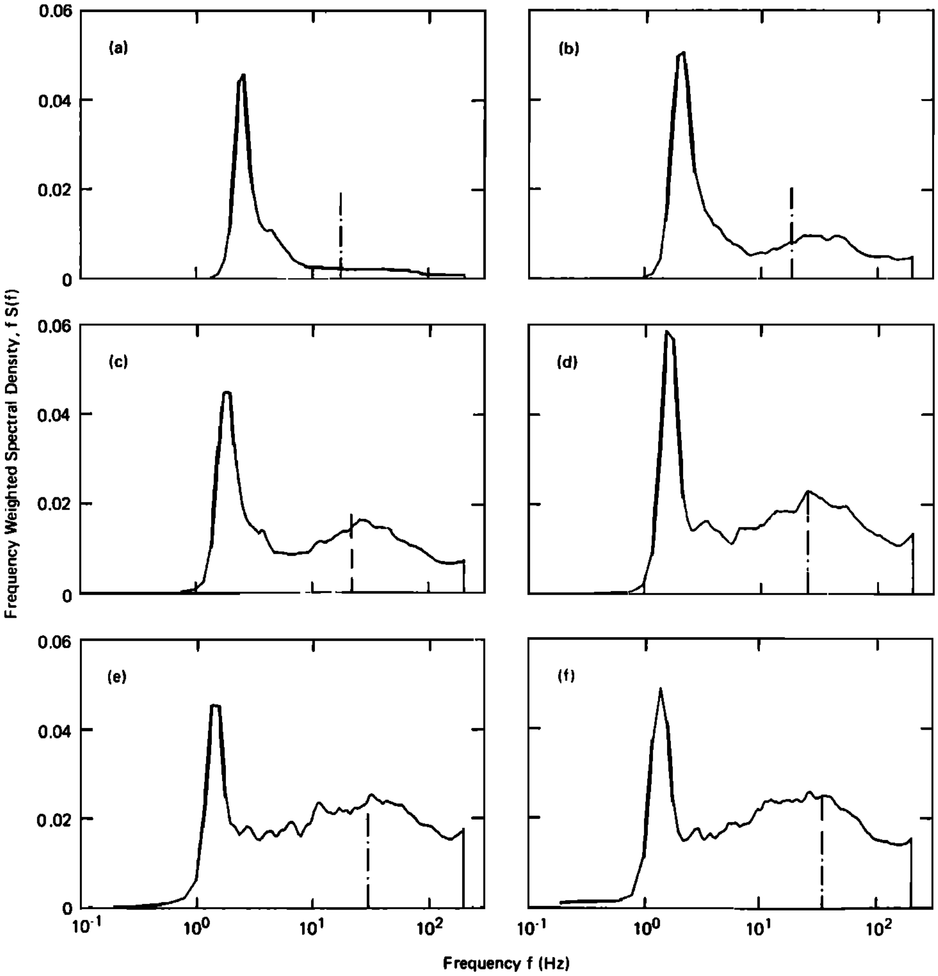

Fig. 6. Area preserving spectra of water-surface slopes under various wind velocities. The data were obtained by Haimbach [1985] at the wind-friction velocity of (*a*) 23, (*b*) 32, (*c*) 42, (*d*) 58, (*e*) 79, and (*f*) 106 cm s^{-1}. The short vertical line divides contributions from gravity and capillary ranges.

slopes. The influence of drift currents on the propagation of surface waves was studied by *Wu* [1975]. For the wave component dividing the gravity and capillary ranges the apparent phase velocity was found to be greater than the actual value by about 0.64 V_s, where V_s is the surface drift current and was found to be about 0.55 u_*. Consequently, we can write

$$(c_m - c_0)/u_* = 0.352 \qquad (10)$$

where $c_0 = 23.2$ cm s^{-1} is the phase velocity of the dividing wave component, and c_m is its corresponding Doppler-shifted value. Substituting values of c_0 and u_* obtained in Haimbach's experiment under various wind velocities into the above expression, we can calculate the apparent frequency of this particular wave component; it is marked as a short vertical line in Figure 6.

For the frequency-weighted spectrum the contribution to the mean square slope is proportional to the area under the curve. Relative contributions of capillary and gravity ranges can now be obtained by comparing two areas divided by the vertical line. The ratios between their contributions obtained from Figure 6 are also shown in Figure 5; the trend of data is indicated by the dashed line. Again, capillary waves make a negligible contribution at very low winds. As the wind velocity increases, its contribution increases rapidly at the wind-friction velocity of about 30 cm s^{-1}. As the wind velocity further increases, the contribution from the capillary range reaches a maximum value of making one half that from the gravity range at the wind-friction velocity of 55 cm s^{-1}. At high winds, both ranges are seen to make comparable contributions.

Different compositions at various fetches

As shown in Figure 5, capillary waves start to make their contribution to the mean square slope sooner at a smaller wind-friction velocity in laboratory tanks than in the field. Relatively little differences in spectral compositions are seen at low winds between fine surface-structures existing in laboratory tanks and the field. Their compositions are distinctly different at high winds, where gravity waves make the main contribution in laboratory tanks, while capillary waves make the main contribution in the field.

The spectrum of wind waves at short fetches is generally more peaked than that for a fully developed sea. A parameter, the so-called enhancement factor, was defined to indicate the degree of peakedness [*Hasselmann et al.*, 1973]; this factor was found to decrease as the fetch increased. The excessive wave energies around the spectral peak, certainly in the gravity range, should make a greater contribution to the mean square slope. In other words, as the fetch increases, the gravity range should make a lesser contribution to the mean square slope; this is consistent with the results shown in Figure 5.

4. QUANTIFICATION OF MEAN SQUARE SLOPES

Composite pictures

Spectral compositions. Compositions of the mean square slope discussed earlier reveal two important results which are not generally recognized: capillary waves do not contribute to the mean square slope at low winds ($U_{10} < 7$ m s^{-1}) in the field, and gravity waves provide the major contribution to the mean square slope at all wind velocities in laboratory tanks. As discussed earlier and shown in Figure 5, the mean square slopes in both laboratory and field are contributed almost exclusively by gravity waves at very low wind velocities, $u_* < 15$ cm s^{-1} in laboratory tanks and $u_* < 25$ cm s^{-1} in the field. Consequently, the mean square slope at very low wind velocities is greater in the field because the spectrum of ocean waves is extended to much lower frequencies. The laboratory value becomes greater at intermediate wind velocities (15 cm s^{-1} $< u_* <$ 25 cm s^{-1}), where capillary waves have already started to make their contribution in laboratory tanks but not in the field. The laboratory value remains to be greater at high wind velocities ($u_* >$ 25 cm s^{-1}) but for a different reason, with the gravity-wave contribution in laboratory tanks fading away much more slowly than that in the field.

Directional distributions. The directional spreading of fine surface structures indicated by the ratio between crosswind and upwind-downwind components in the field has distinctly different variation with the wind velocity from that in laboratory tanks. Leaving aside for the time being the results of *Tang and Shemdin* [1983], the $\overline{s_c^2}/\overline{s_l^2}$ ratio is seen in Figures 1*d* and 1*e* to be almost invariant with the wind velocity in the field. On the other hand, this ratio is seen in Figure 2*b* to increase distinctly with the wind velocity in laboratory tanks. The difference is, of course, associated with the spectral composition of the mean square slope. The mean square slope is contributed by short-wave components occupying the high-frequency end of the spectrum; the latter is generally near a state of saturation varying only slightly with the wind velocity. Consequently, the ratio $\overline{s_c^2}/\overline{s_l^2}$ in the field is almost invariant with wind velocity, as the frequency of saturated portion of the spectrum is quite far away from that at the peak of elevation spectrum associated with dominant waves. On the other hand, the frequency range of these short waves is quite close to that at the spectral peak associated with dominant waves in laboratory tanks. Inasmuch as the structure of dominant waves varies rapidly with the wind velocity, the directional spreading of fine surface structures in laboratory tanks varies accordingly.

Summary. In resolving discrepancies between reported laboratory and field results we must first recognize that varied contributions by capillary and gravity wave components prevail in different experimental conditions. Following the above discussion, we further realize that differences in the directional spreading of fine surface structures are caused by the proximity in frequencies of fine surface structures and dominant waves in laboratory tanks and by the disparity in those frequencies in the field. Therefore discrepancies among laboratory results and between laboratory and field results are expected. Furthermore, because of heavy contributions of the gravity range to the mean square slope in laboratory tanks, additional discrepancies are also expected among laboratory results. Even though they were compared on the basis of wind-friction velocity, the development of gravity-wave structures differs in tanks having different dimensions.

Laboratory results

Directional spreading. As discussed above, the discrepancy in mean square slopes obtained in various facilities may be attributed to differences in the development of long waves. Variations in the mean square slope can be associated with structures of long waves or indirectly through their interactions with ripples. Despite this the ratios of $\overline{s_c^2}/\overline{s_l^2}$ from all studies are seen in Figure 2*b* to follow a similar trend to increase with the wind-friction velocity. Excluding those few data points at very low winds with $u_* < 15$ cm s^{-1}, the data can be approximated rather closely by the straight line drawn in the figure and expressed as

$$\overline{s_c^2}/\overline{s_l^2} = 0.30 \ln u_* - 0.67 \tag{11}$$

in which the wind-friction velocity is in centimeters per second.

Mean square slopes. The mean square slopes from all studies are seen in Figure 2*a* to vary with the logarithm of wind-friction velocity. A very similar trend was followed by data sets reported by *Wu* [1977], *Haimbach* [1985], and *Haimbach and Wu* [1986]. This is very encouraging to see, especially because of the facts that different instruments were used by them and that the last two sets of data obtained in the same tank are in a rather close agreement. The first set obtained in a different tank, provides a larger value than the last two; this is expected, as contributions from the gravity range varying with facilities were discussed previously. The data of *Long and Huang* [1976] have a distinctly different variation, showing a two-tier, step-type variation; more studies are needed to confirm and understand these features.

Two solid lines are drawn in Figure 2*a* with one representing the results of *Wu* [1977] and the other the results of *Haimbach* [1985] and *Haimbach and Wu* [1986]. The lines are actually parallel, indicating the same rate of variation of the mean square slope with wind-friction velocity. The lines can be expressed, respectively, as

$$\begin{aligned} \overline{s^2} &= 0.078 \ln u_* - 0.205 \\ \overline{s^2} &= 0.078 \ln u_* - 0.240 \end{aligned} \tag{12}$$

herein the wind-friction velocity is also in centimeters per second. Again, these results are complimentary to each other, as the difference in numerical values is expected due to different long-wave structures in two tanks.

Directional distribution. The directional distribution of mean square slopes has been suggested by *Haimbach and Wu* [1986] to follow

$$\overline{s_\theta^2} = \overline{s_l^2}/[\cos^2\theta + (\overline{s_l^2}/\overline{s_c^2})\sin^2\theta] \tag{13}$$

where $\overline{s_\theta^2}$ is the mean square slope at an angle θ from the wind direction, and $\overline{s_l^2}$ and $\overline{s_l^2}/\overline{s_c^2}$ can be obtained from (11) and (12).

Oceanic results

Directional spreading. Rather consistent trends are seen between the field data reported by *Cox and Munk* [1956] and *Hughes et al.* [1977]. The results of *Tang and Shemdin* [1983], however, show a very different trend, with the crosswind component being generally greater than the upwind-downwind component. Such unusual results indicate either that the wind direction was not accurately determined or that disturbances produced by the wave follower were indeed substantial as suggested by *Dobson* [1985]. As mentioned previously, shapes of the wave-height spectrum whether or not it had a well-defined peak or multiple peaks cannot be used to explain the discrepancy, as there was only one set of data having double peaks. Moreover, this particular spectrum obtained at U_{10} = 6.3 m s^{-1} and shown in Figure 6*a* of *Tang and Shemdin* [1983] is very questionable, as it contained energy levels unreasonably low, even much less than that obtained at a quite smaller wind velocity of U_{10} = 3.5 m s^{-1} and shown in Figure 6*b* of their article. All the other cases classified by them as the "mixed sea" actually should be in the "well-defined peak" category.

Excluding the set of results reported by *Tang and Shemdin* [1983], we see in Figures 1*d* and 1*e* that the ratio between crosswind and upwind-downwind components varies between 0.6 and 1.0 with an

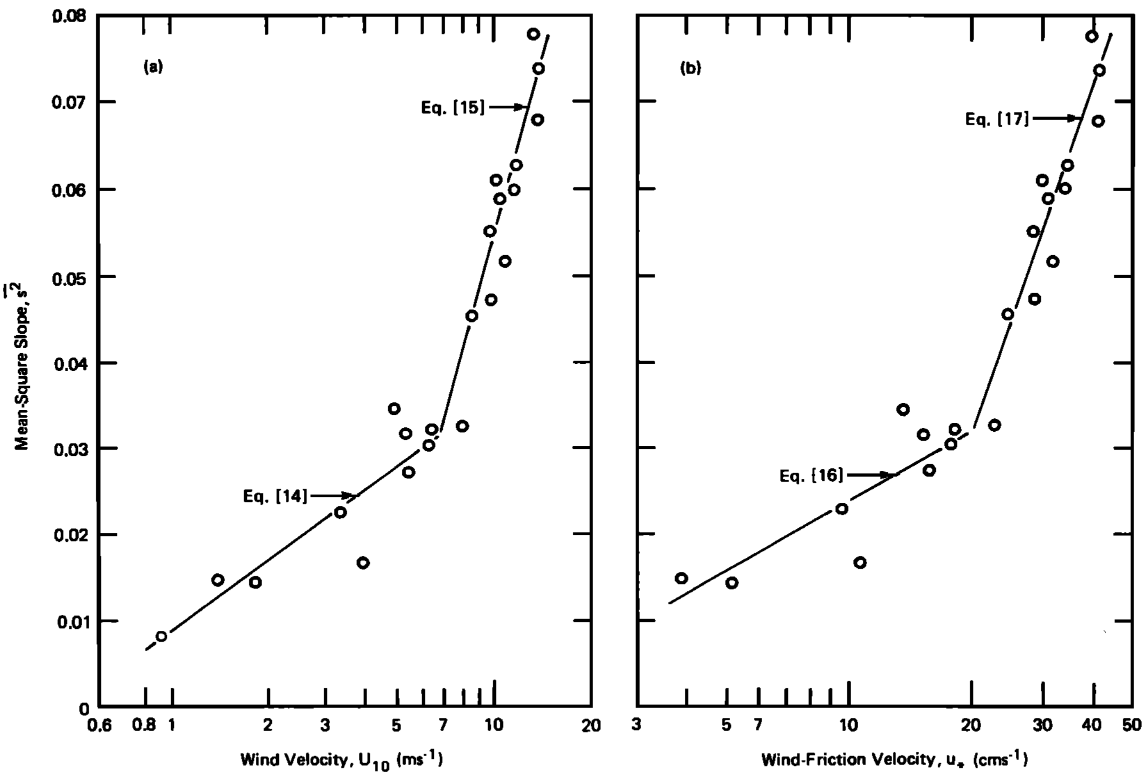

Fig. 7. Variations of mean square slopes with wind and wind-friction velocities. The data are from *Cox and Munk* [1956].

average value of 0.8 for the results of *Cox and Munk* [1956] and between 0.6 and 0.8 with an averaging value of 0.7 for the results of *Hughes et al.* [1977]. The results of Cox and Munk were obtained at a much wider range of wind velocities; in addition, disturbances introduced by the research vessel and the instrument support and effects of the atmospheric stability in the experiments of Hughes et al. still need to be evaluated. We therefore choose at this stage to adopt the ratio $\overline{s_c^2}/\overline{s_l^2}$ to be 0.8. There are, of course, some finer trends in Cox and Munk's results showing the variation of this ratio with wind velocity; they are left for future studies.

Mean square slopes. As discussed earlier in terms of the directional wave spectrum, the variation of the mean square slopes obtained by Cox and Munk with wind velocity should follow a two-segment trend divided at $U_{10} = 7$ m s^{-1}; in each region the mean square slope should vary with the logarithm of wind velocity. The data of Cox and Munk are replotted in a linear-log form in Figure 7*a*, in which one of the data points that deviates very clearly from the rest of the data was removed. Straight lines were fitted as shown in the figure to various segments of the data. For low winds ($U_{10} <$ 7 m s^{-1}) we have

$$\overline{s^2} = (0.90 + 1.20 \ln U_{10}) \times 10^{-2} \tag{14}$$

and for high winds ($U_{10} > 7$ m s^{-1}) we have

$$\overline{s^2} = (-8.40 + 6.00 \ln U_{10}) \times 10^{-2} \tag{15}$$

herein U_{10} is in meters per second. The above expressions appear to provide a better fit to the data than those proposed earlier [*Wu*, 1972].

The results shown in Figure 7*a* were presented versus wind velocities; they should follow the presentation of laboratory results shown in Figure 2 using the wind-friction velocity as the reference parameter. The corresponding wind-friction velocities were calculated earlier; variations of the mean square slope with the wind-friction velocity are presented in Figure 7*b*. Again, the data are seen to follow a two-segment variation illustrated by straight lines drawn in the figure. For low winds ($u_* < 20$ cm s^{-1}) we have

$$\overline{s^2} = (1.15 \ln u_* - 0.275) \times 10^{-2} \quad (16)$$

and for high winds ($u_* > 20$ cm s^{-1}) we have

$$\overline{s^2} = (5.86 \ln u_* - 14.40) \times 10^{-2} \quad (17)$$

where u_* is expressed in centimeters per second.

Directional distributions. The directional distribution of mean square slopes of the sea surface should also follow the same functional form shown in (12) with two components of the mean square slopes shown in (14)–(17), $\overline{s_c^2}/\overline{s_l^2} = 0.8$ adopted in the last section, and $\overline{s_l^2} = \overline{s^2}/1.8$.

5. CONCLUDING REMARKS

Many sets of measurements on the mean square slope of wind-disturbed water surface were performed in laboratory tanks and the field. Previous users were confused by discrepancies in their results, not only between two groups but also with each group. Consequently, it was difficult to choose among them. Our analyses in resolving those discrepancies therefore provide useful formulae for both laboratory and field applications. In addition, these results also provide insights on mechanisms governing the development of fine sea-surface structures.

Acknowledgments. The author is very grateful for sponsorships of his work provided by the Radar Division, Naval Research Laboratory (N00173-88-M-7140), the Physical Oceanography Program, National Science Foundation (OCE 8716519), and the Fluid Dynamics Program, Office of Naval Research (N00014-89-J-1100).

REFERENCES

Cox, C. S., Measurements of slopes of high-frequency wind waves, *J. Mar. Res.*, *16*, 199–225, 1958.

Cox, C. S., and W. H. Munk, Slopes of the sea surface deduced from photographs of sun glitter, *Bull. Scripps Instit. Oceanogr.*, *6*, 9, 1956.

Dobson, F., Comment on "Measurement of high-frequency waves using a wave follower" by S. Tang and O. H. Shemdin, *J. Geophys. Res.*, *90*, 9203–9204, 1985.

Haimbach, S. P., Development of slope spectra of the wind-disturbed water surface, doctoral dissertation, Univ. of Del., Newark, 1985.

Haimbach, S. P., and J. Wu, Field trials of an optical scanner for studying sea-surface fine structures, *IEEE J. Oceanic Eng.*, *OE-10*, 451–453, 1985.

Haimbach, S. P., and J. Wu, Directional slope distributions of wind-disturbed water surface, *Radio Sci.*, *21*, 73–79, 1986.

Hasselmann, K., et al., Measurements of wind-wave growth and swell decay during the Joint North Sea Wave Project (JONSWAP), *Reihe A*(12), 95 pp., Herausgegeben vom Deutsch-Hydrograph Inst., Hamburg, Federal Republic of Germany, 1973.

Hughes, B. A., H. L. Grant, and R. W. Chappell, A fast response surface-wave slope meter and measured wind-wave moments, *Deep Sea Res.*, *24*, 1211–1223, 1987.

Kitaigorodskii, S. A., On the theory of the equilibrium range in the spectrum of wind-generated gravity waves, *J. Phys. Oceanogr.*, *13*, 816–827, 1983.

Long, S. R., and N. E. Huang, On the variation and growth of wave-slope spectra in the capillary-gravity range with increasing wind, *J. Fluid Mech.*, *77*, 209–228, 1976.

Longuet-Higgins, M. S., On wave breaking and the equilibrium spectrum of wind-generated waves, *Proc. Roy. Soc.*, *A310*, 150–159, 1969.

Moore, R. K., Radar sensing of the ocean, *IEEE J. Oceanic Eng.*, *OE-10*, 84–112, 1985.

Phillips, O. M., *The Dynamics of the Upper Ocean*, Cambridge University Press, New York, 1977.

Phillips, O. M., Spectral statistical properties of the equilibrium range in the wind-generated gravity waves, *J. Fluid Mech.*, *156*, 506–531, 1985.

Scully-Power, P., Navy oceanography shuttle observations, *Mission Rep. STS 41-G*, Navy Underwater Sys. Cent., Newport, R. I., 1986.

Tang, S., and O. H. Shemdin, Measurement of high-frequency waves using a wave follower, *J. Geophys. Res.*, *88*, 9832–9840, 1983.

Toba, Y., Local balance in the air-sea boundary processes, 3, On the spectrum of wind waves, *J. Oceanogr. Soc. J.*, *29*, 209–220, 1973.

Wu, J., Slope and curvature distributions of wind-disturbed water surface, *J. Opt. Soc. Am.*, *61*, 852–858, 1971.

Wu, J., Sea surface slope and equilibrium wind-waves spectra, *Phys. Fluids*, *15*, 741–747, 1972.

Wu, J., Wind-induced drift currents, *J. Fluid Mech.*, *68*, 49–70, 1975.

Wu, J., Directional slope and curvature distributions of wind waves, *J. Fluid Mech.*, *79*, 463–480, 1977.

Wu, J., Wind-stress coefficients over sea surface near neutral conditions, A revisit, *J. Phys. Oceanogr.*, *10*, 727–740, 1980.

Wu, J., Parameterization of wind-stress coefficients over water surface, *J. Geophys. Res.*, *90*, 9069–9072, 1985.

Wu, J., Stability parameters and wind-stress coefficients under various atmospheric conditions, *J. Atmos. Oceanic Tech.*, *3*, 333–339, 1986.

Wu, J., Suppression of oceanic ripples by surfactant, Spectual effects deduced from sun-glitter, wave-staff and microwave measurements, *J. Phys. Oceanogr.*, *19*, 238–245, 1989.

J. Wu, Air-Sea Interaction Laboratory, College of Marine Studies, University of Delaware, Lewes, DE 19958.